

In-situ analysis of a boron-based catalytic electrode with trace platinum for efficient hydrogen evolution in a wide pH range

Xunwei Ma^{a,b#}, Yifan Zhang^{a#}, Liugang Wu^a, Zijun Huang^a, Jiyuan Yang^d, Chunguang Chen^a, Shengwei Deng^e, Lincai Wang^{b*}, Jian Chen^{c*}, Weiju Hao^{a*}

^aUniversity of Shanghai for Science and Technology, Shanghai 200093, P. R. China E-Mail:
wjhao@usst.edu.cn

^bSchool of Resources and Environmental Engineering, Shanghai Polytechnic University, Shanghai
201209, P. R. China E-Mail: lcwang@sspu.edu.cn

^cDepartment of Orthopedics, Shanghai General Hospital, Shanghai Jiaotong University School of
Medicine, Shanghai Jiaotong University, Shanghai 200080, China. E-Mail:
chenjianpumch@163.com

^dDepartment of Materials Science and Engineering, National University of Singapore, Singapore.

^eCollege of Chemical Engineering, Zhejiang University of Technology, Hangzhou, Zhejiang 310014,
P. R. China

These authors are equal to this work.

1 Characterizations.

The electrochemical workstation (CHI 760E) was used to characterize the electrochemical performance of materials, the scanning electron microscope (SEM, JEOL JSM 7001F) was used to observe the micro morphology and structure of materials, the energy-dispersive X-ray spectrometer (EDS) was used to analyze the types and content of elements in material micro-regions, the X-ray photoelectron spectrometer (XPS, Thermo Scientific K-Alpha) was used to analyze the surface element composition and chemical states of materials, the X-ray diffraction instrument (XRD, Bruker D8 ADVANCE) was used to explore crystal structures, the transmission electron microscope (TEM, Tecnai TF20) was used to analyze the micro morphology and structure of materials, the high-resolution transmission electron microscope (HRTEM) was used to observe internal crystal structures, the selected area electron diffraction (SAED) was used to analyze the morphology features and crystallographic properties of crystal samples, the Fourier transform infrared spectrometer (FT-IR, Thermo Fisher Scientific Nicolet iS20) was used to characterize the molecular structure and chemical bonds of materials, the contact angle goniometer (JC2000C1) was used to determine the hydrophilicity of materials, and the programmable DC power supply (PLD-3010) provided voltage and current.

2 Electrochemical measurements.

Using the electrochemical workstation (CHI 760E), electrochemical tests could be conducted under the standard three-electrode system. Here, the counter electrode, reference electrode, and working electrode were carbon rod, saturated calomel electrode (Hg/Hg_2Cl_2), and electrode ($1.0\text{ cm} \times 0.5\text{ cm}$), respectively. The electrolytes used were an alkaline solution (1.0 M KOH) and a neutral high-salt medium (1.0 M NaCl). All potential values were calibrated against the reversible hydrogen electrode (vs. RHE), and calculations were performed as described in equations (1) and (2)¹.

$$E(\text{vs.RHE}) = E(\text{vs.SCE}) + E(Hg/Hg_2Cl_2) + 0.05917 \cdot pH \quad (1)$$

$$\eta = b \times \log|j| + a \quad (2)$$

Here, $E(\text{Hg/Hg}_2\text{Cl}_2) = 0.2415\text{V}$ (at 298 K), η represented the overpotential (mV), b represented Tafel slope (mV dec^{-1}), j represented current density (mA cm^{-2}), and a represented exchange current density.

2.1 Linear sweep voltammetry (LSV).

Set the scan rate to 5 mV s^{-1} , with a scan potential range from -1.0 V to -1.6 V (vs. SCE) for testing the hydrogen evolution reaction (HER) under alkaline conditions (1.0 M KOH), and from -0.6 V to -1.2 V (vs. SCE) for testing HER under neutral conditions (1.0 M NaCl).

2.2 Electrochemical impedance spectroscopy (EIS).

Set the frequency range to 10^5 -1 Hz, AC amplitude to 5 mV, and perform electrochemical impedance spectroscopy (EIS) to calculate the charge transfer resistance (R_{ct}).

2.3 Electrochemical active surface area (ECSA) and Cyclic voltammetry (CV).

Cyclic Voltammetry (CV) could evaluate the electrochemical active surface area (ECSA) by analyzing the induced current density at different scan rates. Perform CV tests at scan rates of 3, 4, 5, 6, and 7 mV s^{-1} in the non-Faradaic region from 0.09 to 0.15 V (vs. RHE). The ECSA could be derived by analyzing the induced current density at different scan rates. By plotting the CV curve, the double-layer capacitance (C_{dl}) could be calculated. The calculation was based on equations (3) and (4)².

$$C_{dl} = \frac{j}{v} \quad (3)$$

$$ECSA = \frac{C_{dl} \times A}{C_s \times m} \quad (4)$$

Here, j represented current density (mA cm^{-2}), v represents scan rate (mV s^{-1}), A represented the exposed surface area of the working electrode (cm^2), C_s represented the specific capacitance (0.040 mF cm^{-2}), and m represented the mass loading of the catalyst (g).

2.4 Stability.

Conduct the potentiostatic time test ($v-t$) by using a DC power supply (PLD-3010). Measure the fluctuation amplitude of overpotential to evaluate the long-term stability of HER under conditions of constant current density.

2.5 Turnover frequency (TOF).

Turnover Frequency (TOF) could evaluate the intrinsic activity of an electrocatalyst. It represented the number of hydrogen molecules converted per unit time on a per active site basis. The calculation was shown in equation (5)³.

$$TOF_{HER} = \frac{j \times A}{2 \times F \times n} \quad (5)$$

Here, j represented current density (mA cm^{-2}), A represented the exposed surface area of the working electrode (cm^2), F represented Faraday's constant (96485 C mol^{-1}), and n represented the molar amount of metal measured *through* ICP-OES. Since the exact number of catalytic sites was difficult to determine, it was commonly assumed that all catalytic species exhibited electrocatalytic activity.

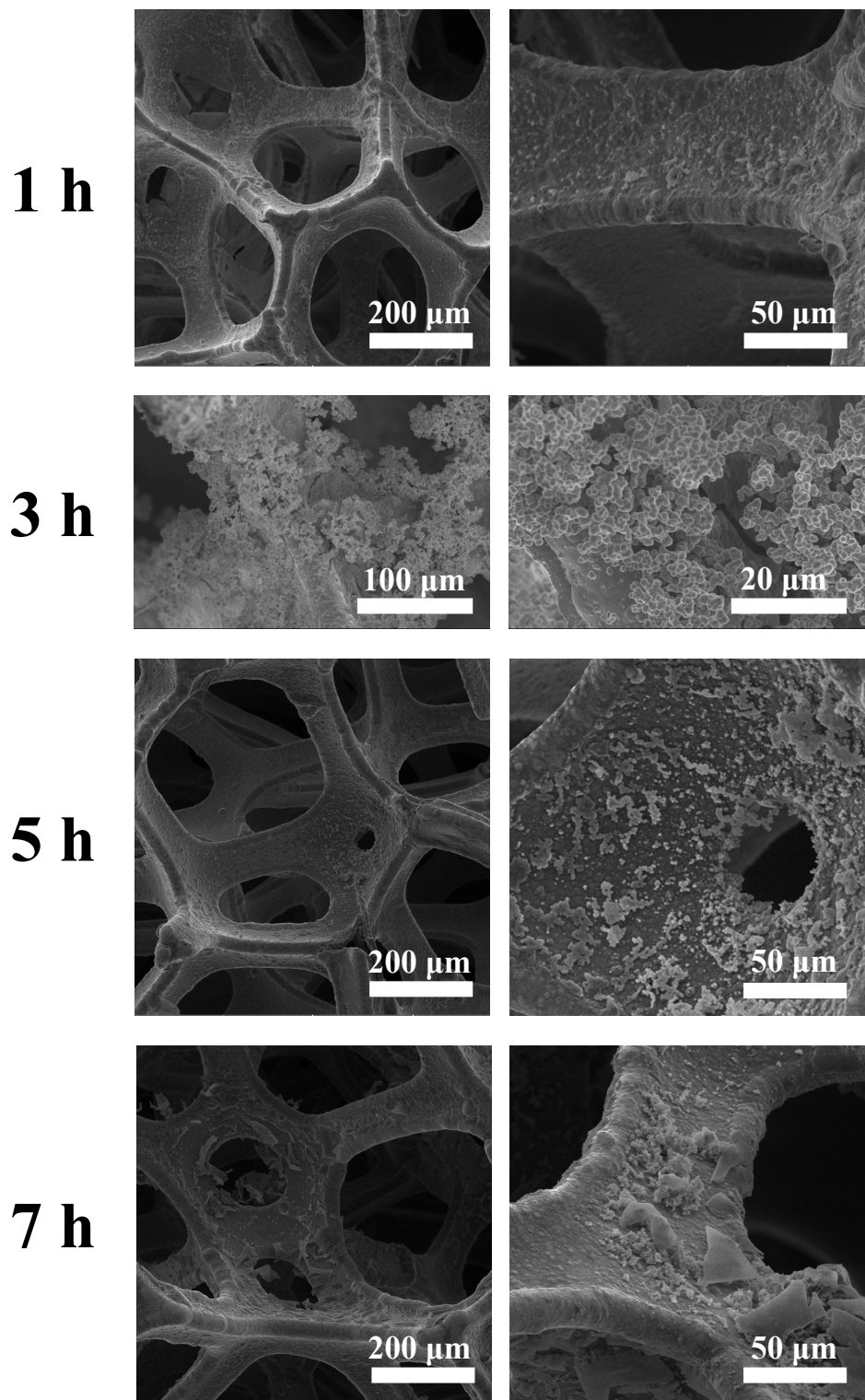


Figure S1 SEM images of NiB@NF with different electroless plating time (1h, 3h, 5h, and 7h).

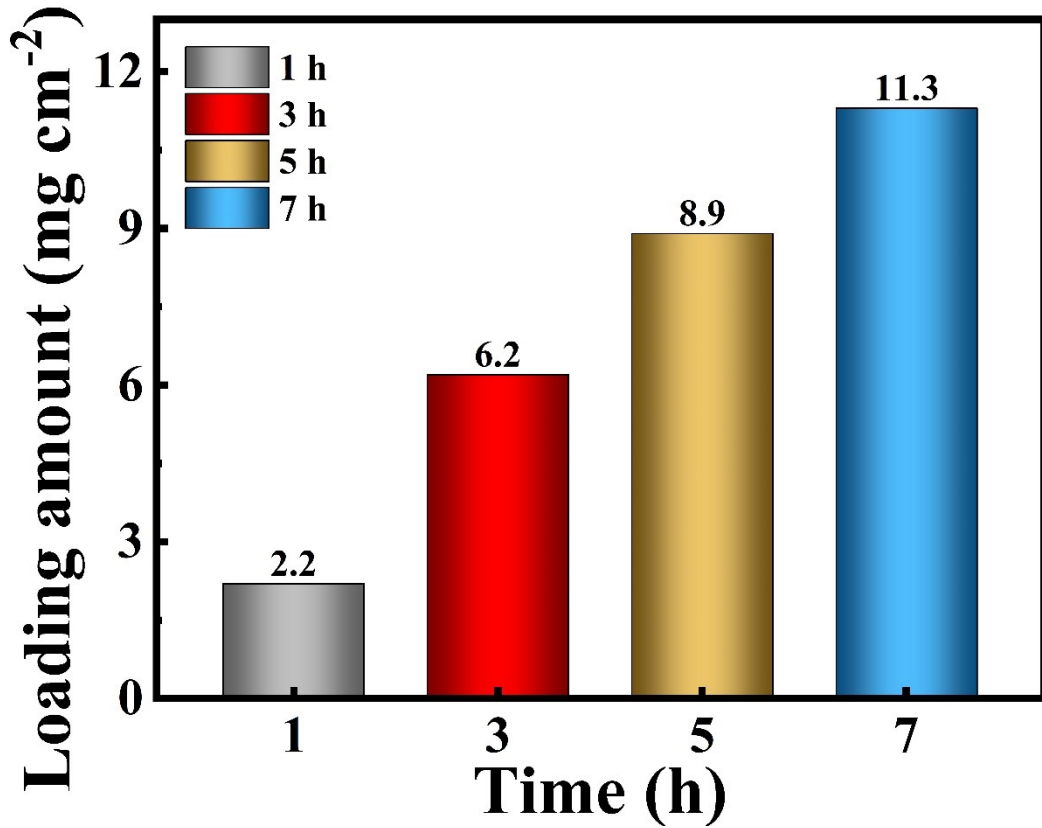


Figure S2 The loading amount of NiB@NF with different electroless plating time.

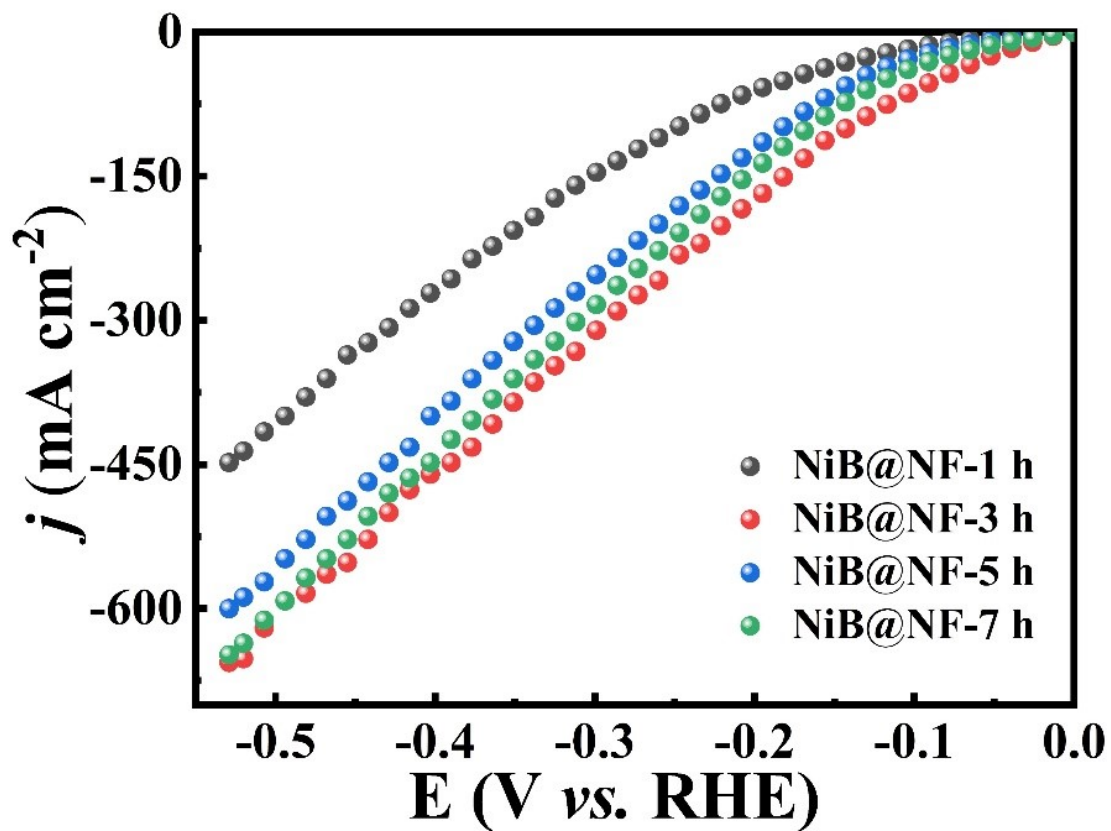


Figure S3 LSV curves of NiB@NF with different electroless plating time during HER process in 1.0 M KOH.

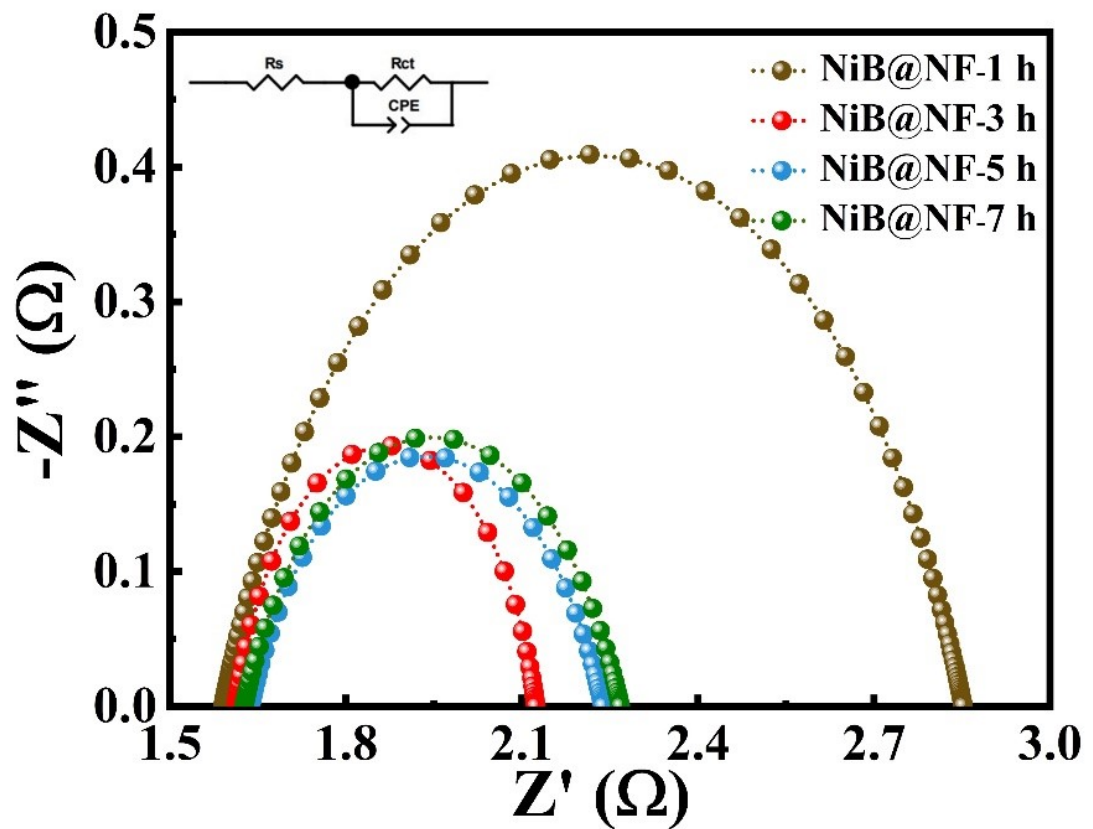
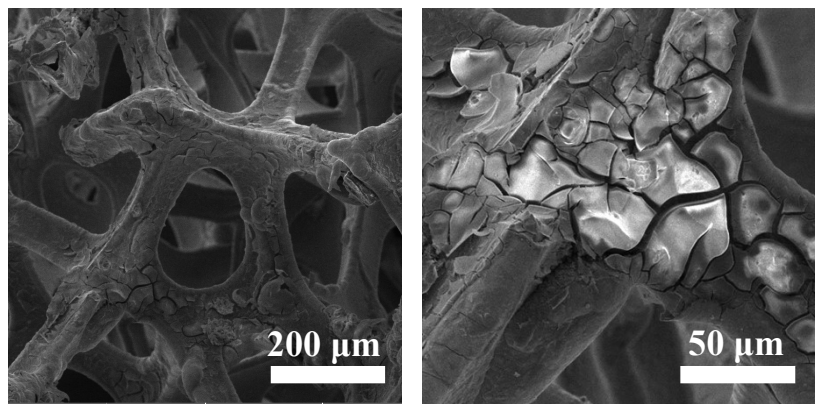
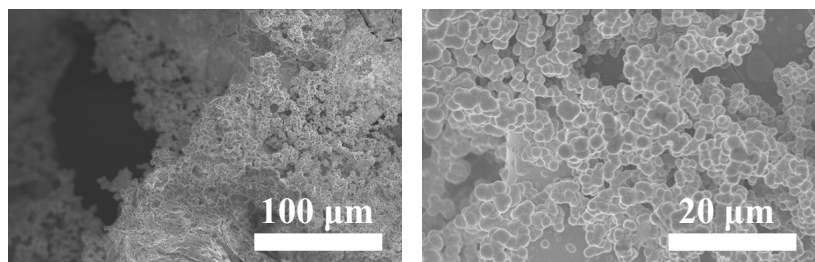


Figure S4 Nyquist plots of NiB@NF electrodes with different electroless plating time in 1.0 M KOH.

1 min



5 min



10 min

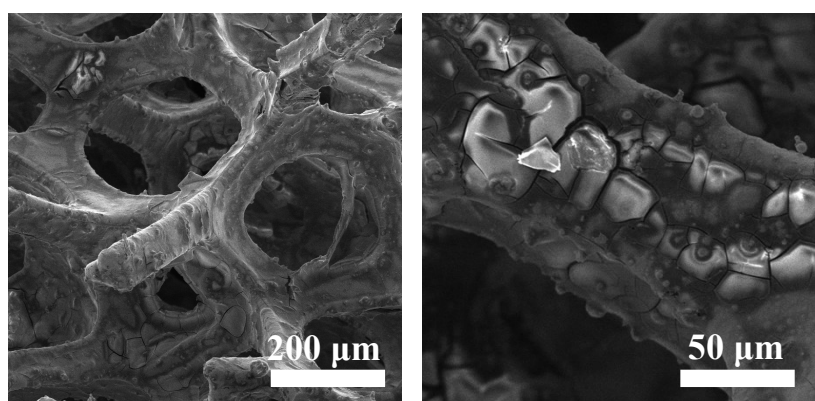


Figure S5 SEM images of Pt-NiB@NF with different electroplating time (1min, 5min, and 10min).

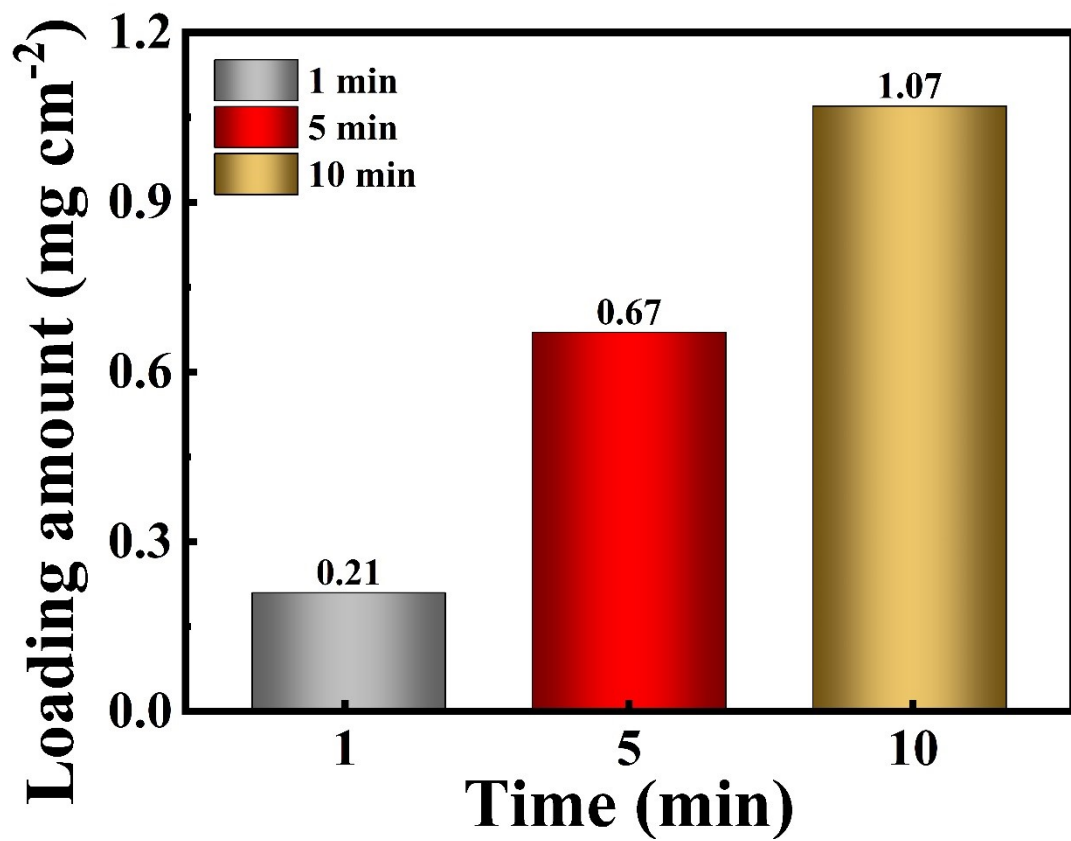


Figure S6 Deposition quality of Pt on NiB@NF precursor at different electroplating times.

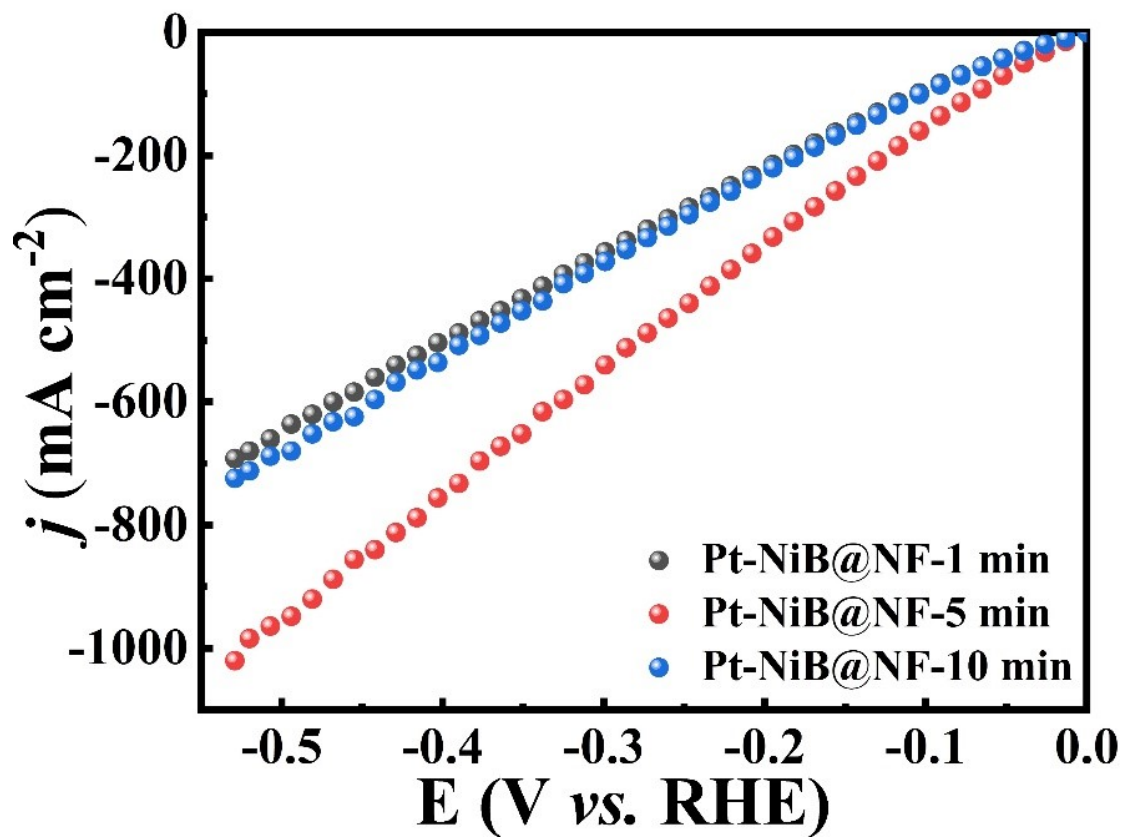


Figure S7 LSV curves of Pt-NiB@NF with different electroplating time during HER process in 1.0 M KOH.

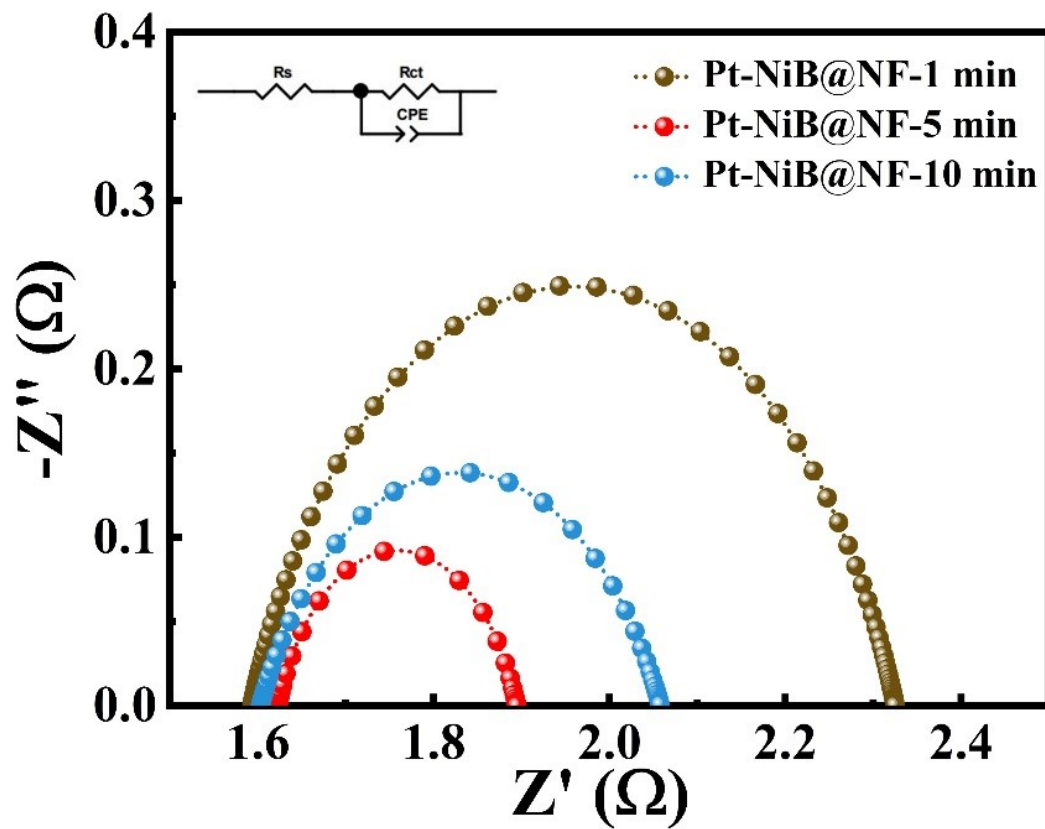


Figure S8 Nyquist plots of Pt-NiB@NF electrodes with different electroplating time in 1.0 M KOH.

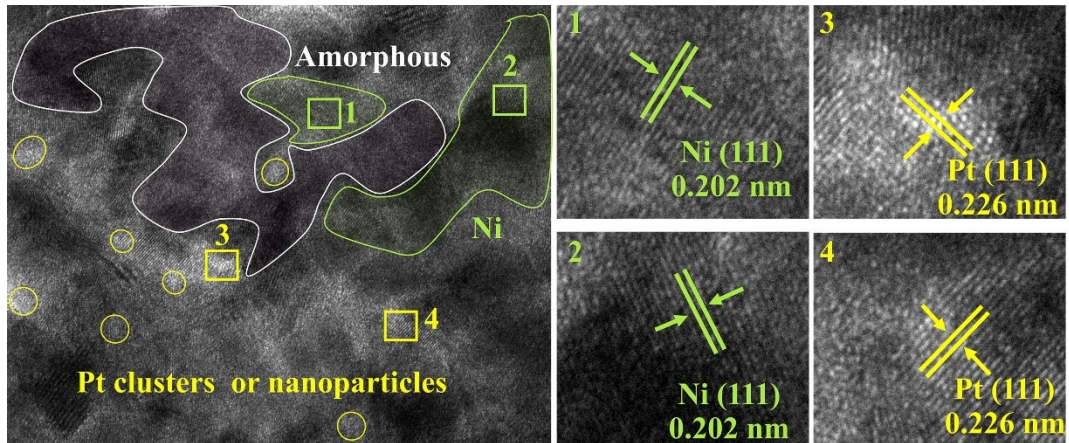


Figure S9 HR-TEM images of Pt-NiB.

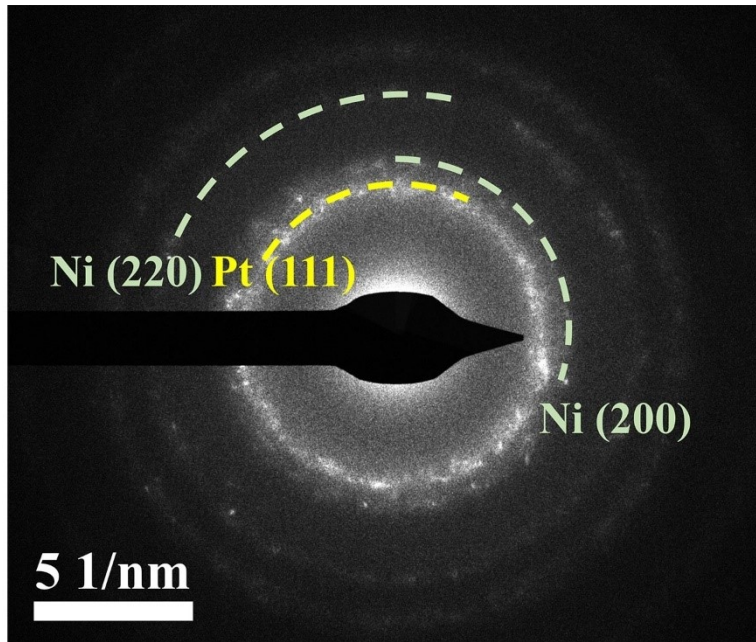


Figure S10 SAED image of Pt-NiB.

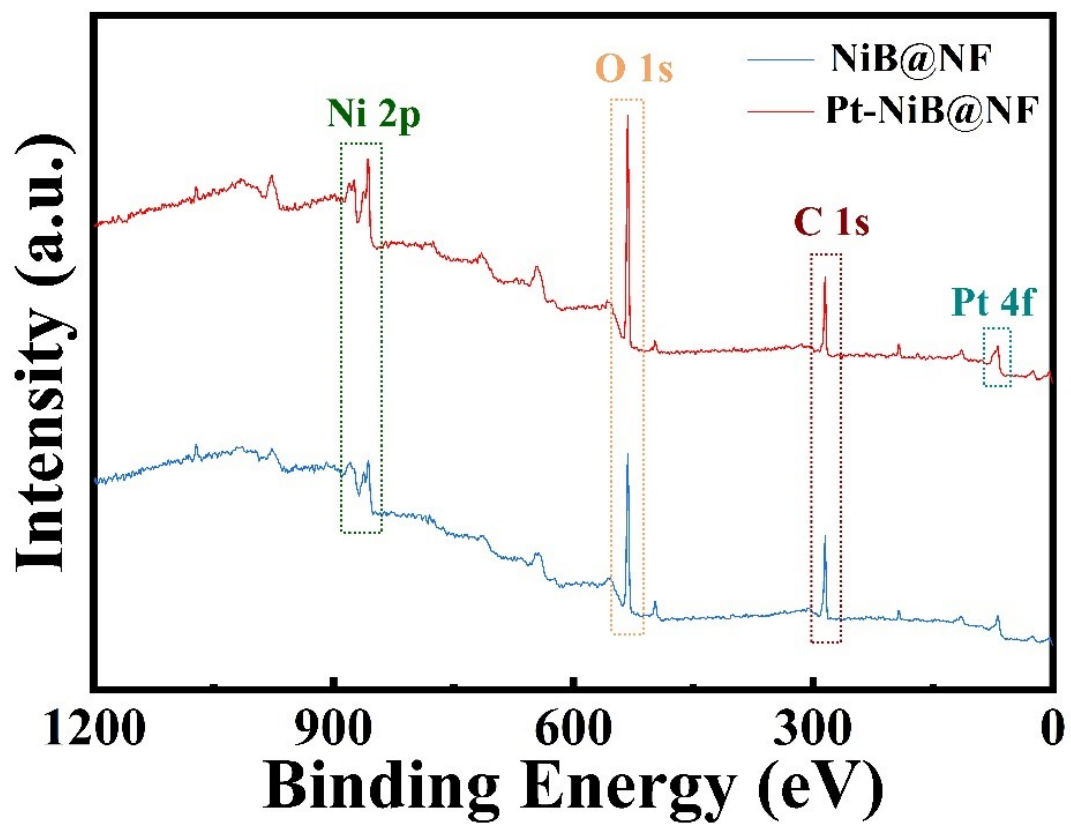


Figure S11 XPS survey spectra of Pt-NiB@NF and NiB@NF

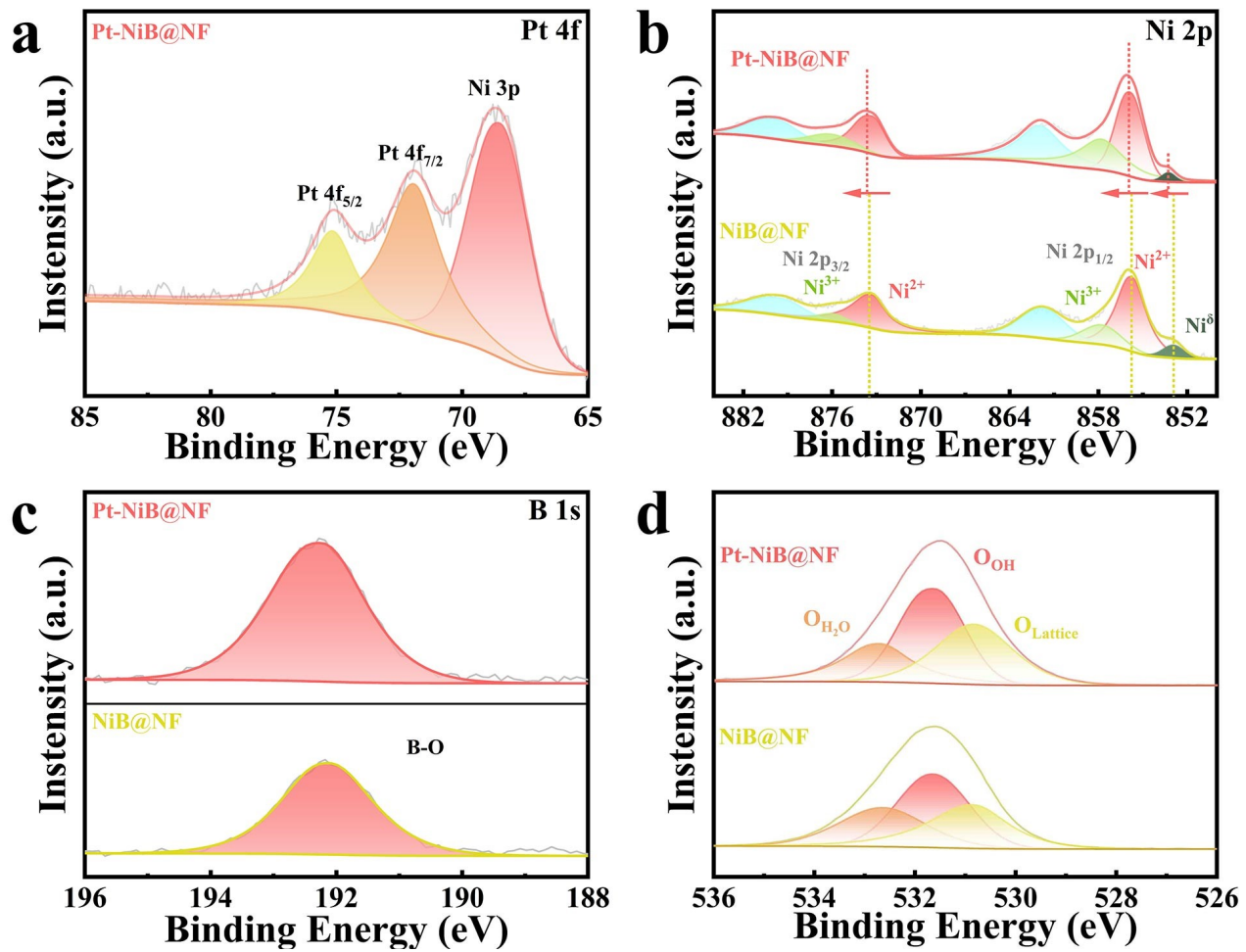


Figure S12 XPS spectra of (a) Pt 4f, (b) Ni 2p,(c) B 1s and (d) O 1s for the Pt-NiB@NF electrode.

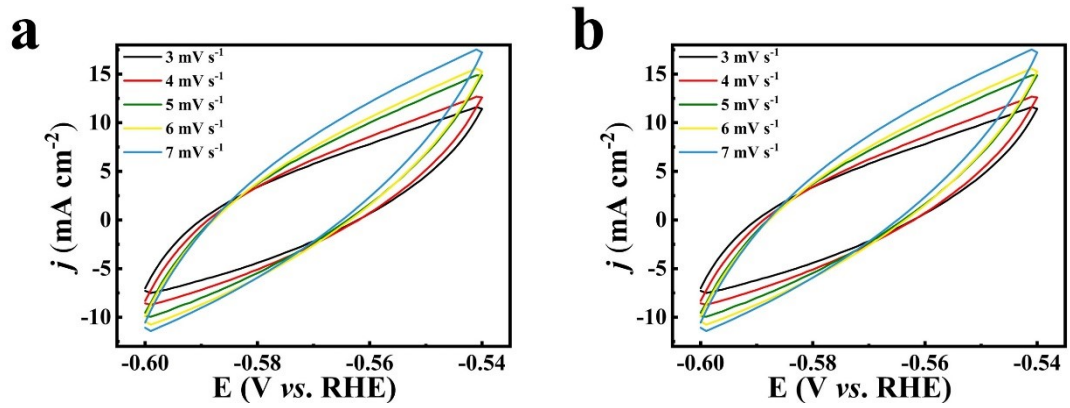


Figure S13 The CV curves at different scan rates of (a) NiB@NF and (b) Pt-NiB@NF electrodes in 1.0 M NaCl.

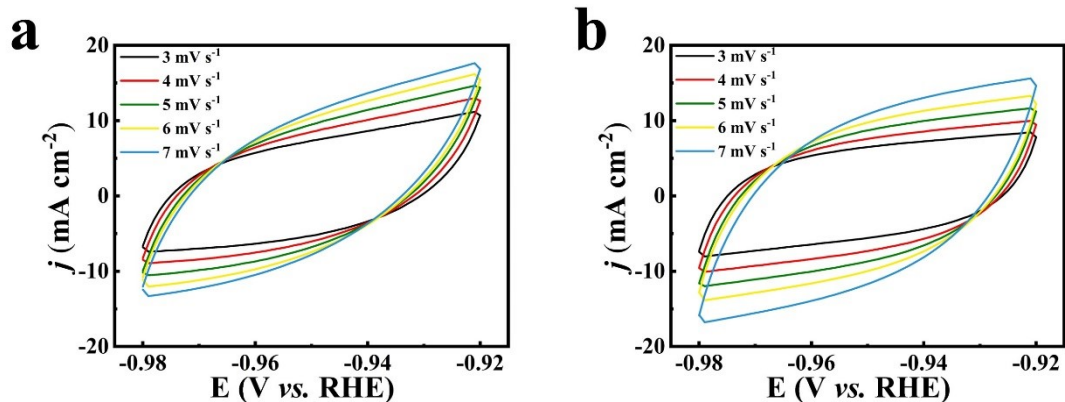


Figure S14 The CV curves at different scan rates of (a) NiB@NF and (b) Pt-NiB@NF electrodes in 1.0 M KOH.

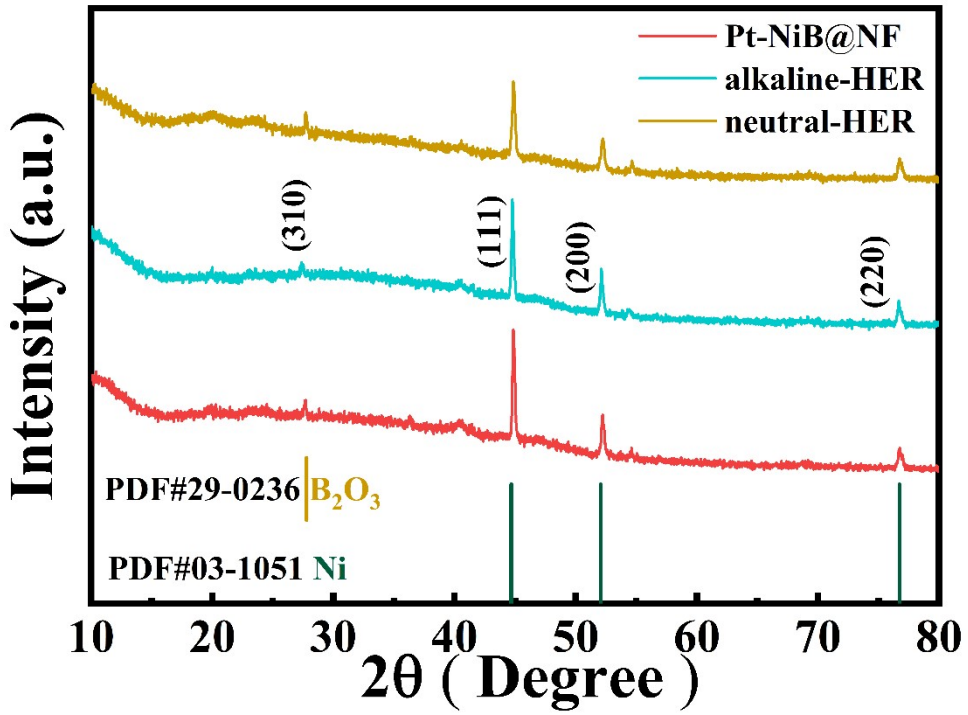


Figure S15 XRD patterns of Pt-NiB@NF and post-HER Pt-NiB@NF in the 1.0 M KOH and 1.0 M NaCl.

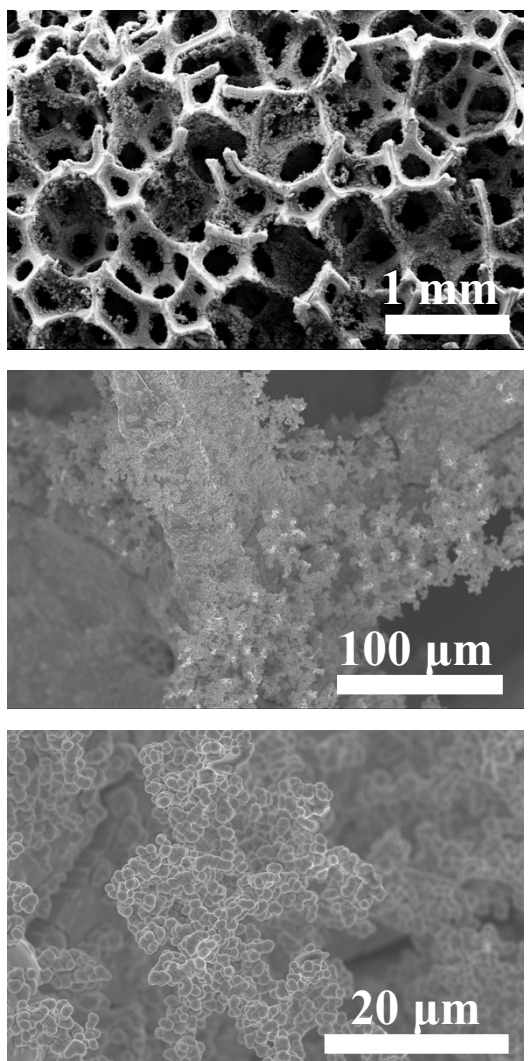


Figure S16 SEM images of post-HER Pt-NiB@NF electrode in 1.0 M NaCl.

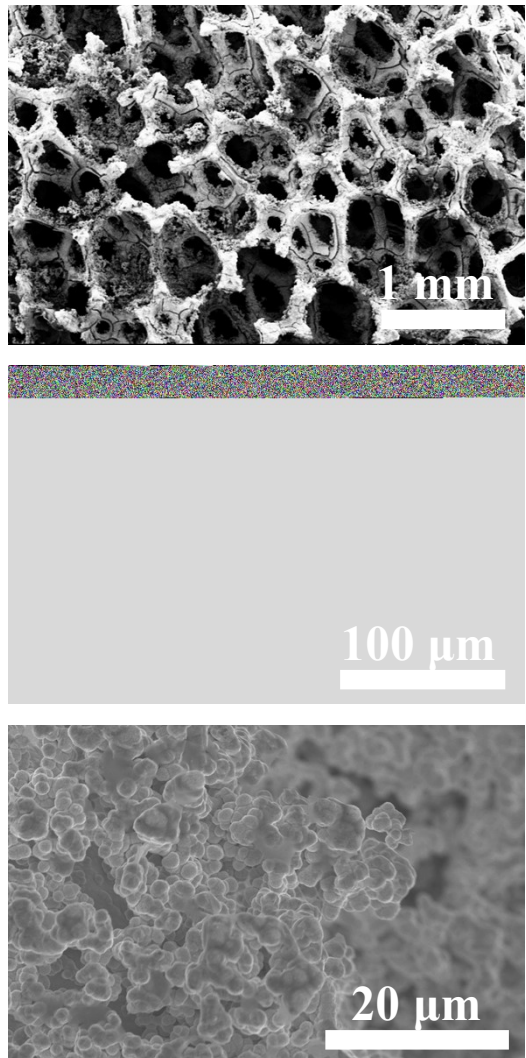


Figure S17 SEM images of post-HER Pt-NiB@NF electrode in 1.0 M KOH.

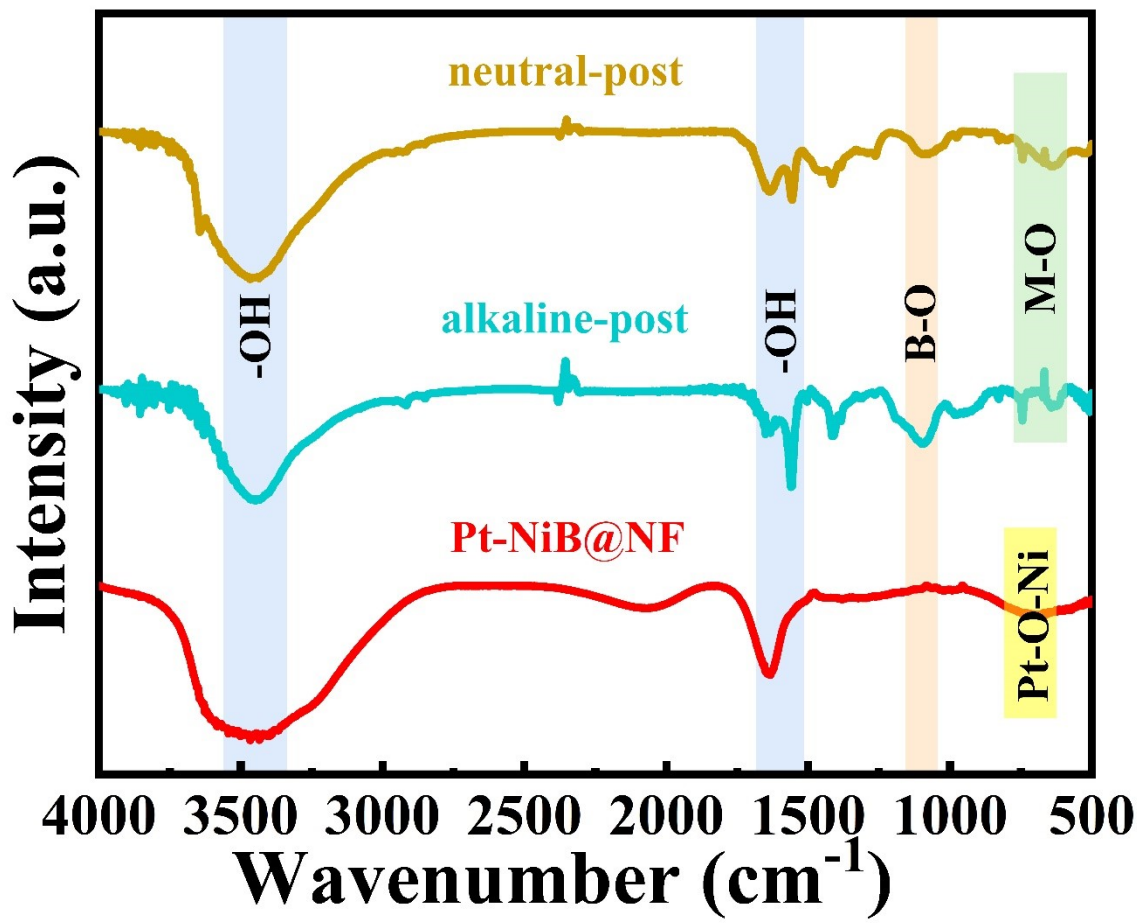


Figure S18 FT-IR spectra of Pt-NiB@NF and post-HER Pt-NiB@NF in the 1.0 M KOH and 1.0 M NaCl.

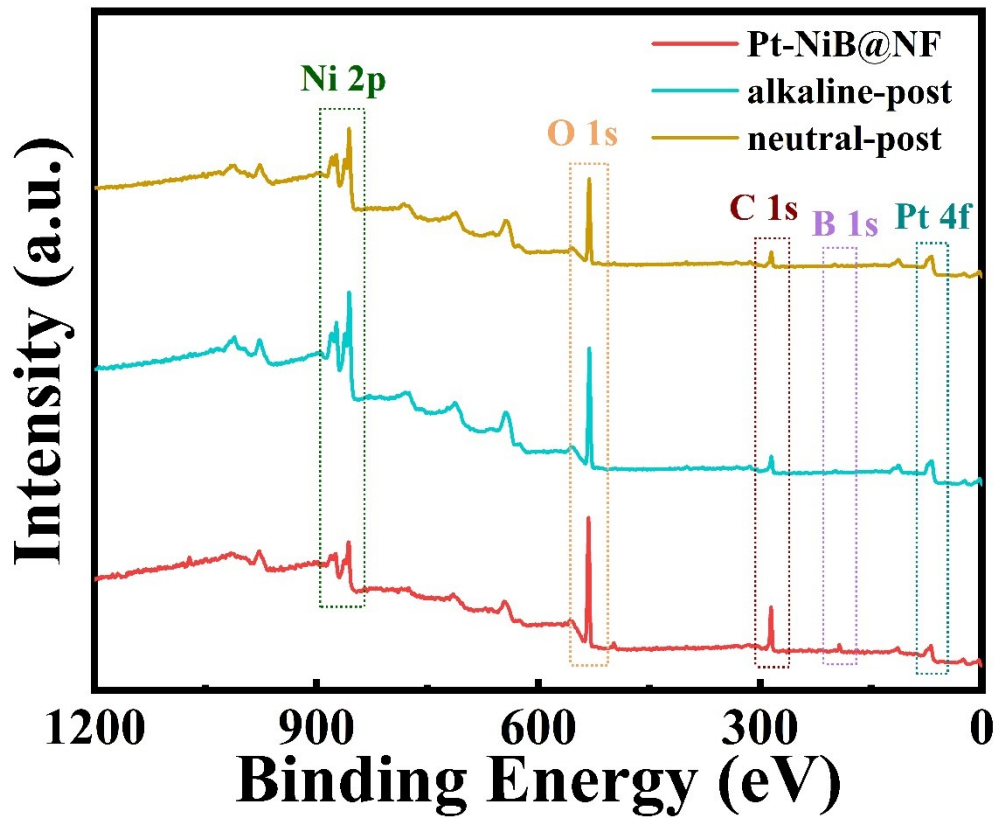


Figure S19 XPS survey spectra of Pt-NiB@NF and it post-HER.

Table S1 ICP-OES results of NiB@NF and Pt-NiB@NF electrodes.

Samples	Ni (wt%)	B (wt%)	Pt (wt%)
NiB@NF	97.80	1.84	0.00
Pt-NiB@NF	95.31	1.66	0.58

Table S2. Comparison of the HER performance of Pt-NiB@NF with other electrocatalysts in neutral solution

Catalyst	Overpotential (η ₁₀ , mV)	Electrolyte	References
Pt-NiB@NF	70	1.0 M NaCl	This work
vs-Ru-Ni ₉ S ₈	131	1.0 M PBS	⁴
Ni ₂ P@B,N-GC	113	1.0 M PBS	⁵
VN/Co-NC	163	1.0 M PBS	⁶
N,Cu-CoP/CC	64.7	1.0 M PBS	⁷
vr-1T MoS ₂	212	1.0 M PBS	⁸
Ru/D-NPC	61.3	1.0 M PBS	⁹
S-MoP/CC	127	1.0 M PBS	¹⁰
Co@CNTs Ru	63	1.0 M PBS	¹¹
CoNi ₂ S ₄ /WS ₂ /Co ₉ S ₈	146	1.0 M PBS	¹²
CuCo-CAT	143	1.0 M PBS	¹³
NiS ₂ -ReS ₂ -V ₁	122	1.0 M PBS	¹⁴
Ru-Cu ₂ O/CF	51	1.0 M PBS	¹⁵
MoP-Ru ₂ P/NPC	126	1.0 M PBS	¹⁶
Cu-Mo ₂ C	78	1.0 M PBS	¹⁷
Ru/Mo ₂ CT _x	73	1.0 M PBS	¹⁸
Ni ₂ P/CoP	65.2	1.0 M PBS	¹⁹
MoS ₂ /NVO-2	68	1.0 M PBS	²⁰
MoN/Co ₄ N	72	1.0 M PBS	²¹
PdSe ₂	138	1.0 M PBS	²²
Fe-Ni ₃ S ₂ @FeNi ₃ -8	83	1.0 M PBS	²³
Ru/RuO ₂ NB/C	68	1.0 M PBS	²⁴
Ru-WO ₃	83	1.0 M PBS	²⁵

Table S3. Comparison of the HER performance of Pt-NiB@NF with other electrocatalysts in alkaline solution

Catalyst	Overpotential (η ₁₀ , mV)	Electrolyte	References
Pt-NiB@NF	12	1.0 M KOH	This work
Ni@IrNi	33	1.0 M KOH	²⁶
NiB/NF	41.2	1.0 M KOH	²⁷
RuIr@BCN	23.6	1.0 M KOH	²⁸
Ru - MnFeP/NF	35	1.0 M KOH	²⁹
Ru-Cu ₂ O/CF	31	1.0 M KOH	¹⁵
NiRu-LDH	38	1.0 M KOH	³⁰
Ni ₂ P@B,N-GC	84	1.0 M KOH	⁵
(c/o)-CoSe ₂ -W	29.8	1.0 M KOH	³¹
NiS ₂ -ReS ₂ -V ₁	49	1.0 M KOH	¹⁴
TRO/RKLTO	20	1.0 M KOH	³²
Ni ₂ P/NiTe ₂ /NF	62	1.0 M KOH	³³
Fe _{0.01} &Mo-NiO	26	1.0 M KOH	³⁴
A-CoB _i /MXene	15	1.0 M KOH	³⁵
Co(OH) ₂ @MXene	21	1.0 M KOH	³⁶
RuO ₂ -300Ar	17	1.0 M KOH	³⁷
Co@CNTs Ru	10	1.0 M KOH	¹¹
CoNi ₂ S ₄ /WS ₂ /Co ₉ S ₈	70	1.0 M KOH	¹²
VN/Co-NC	44	1.0 M KOH	⁶
CuCo-CAT	52	1.0 M KOH	¹³
MoP-Ru ₂ P/NPC	47	1.0 M KOH	¹⁶
Ru _{1-n} -NC	14.8	1.0 M KOH	³⁸
Ru/D-NPC	23	1.0 M KOH	⁹
S-MoP/CC	75	1.0 M KOH	¹⁰

Table S4. Comparison of the HER performance of Pt-NiB@NF with other Pt-Loading electrocatalysts in neutral solution

Catalyst	Pt loading(wt%)	Overpotential (η_{10} , mV)	References
Pt-NiB@NF	0.58	70	This work
Mo ₂ C@NC@Pt	7.49	25	³⁹
CS-PdPt	4.942	50	⁴⁰
V-NiFeMo LDH	2.23	89	⁴¹
Pt – Co(OH) ₂ /CC	5.7	84	⁴²
YS-Pt-CoP	3.91	88	⁴³
PtCoMo@NC	4.7	66	⁴⁴
Pt@NOMC-A	7.2	65	⁴⁵
Pt-TiO ₂ -x NSs	10	88	⁴⁶
Pt/N-Mo ₂ C	1.08	49	⁴⁷
PtCu – MoO ₂ @C	11.3	131	⁴⁸
Pt ₃ Fe/BNC	13.2	72	⁴⁹
Pt ₃ Fe/NMCS-A	10.3	48	⁵⁰
Pt@CuFe-LDHm	1.1	120	⁵¹
Pt/np-Co _{0.85} Se	1.03	55	⁵²
Pt/PtTe ₂ /NiCoTe ₂ /NPFC HFSs	8.44	36	⁵³
PtP ₂ @PNC	3.5	64	⁵⁴
Pt/VC-2.84	2.84	68	⁵⁵
Ni0.5-NCNFs-Pt	8.3	84	⁵⁶

Table S5. Comparison of the HER performance of Pt-NiB@NF with other Pt-based electrocatalysts in alkaline solution

Catalyst	Pt loading(wt%)	Overpotential (η_{10} , mV)	References
Pt-NiB@NF	0.58	12	This work
Pt/Ni-PCNFs-50	4.3	46	57
Pt/Mo ₆ S ₈	6.73	124	58
Mo ₂ C@NC@Pt	7.49	47	39
PtNi ₅ -0.3	46	26.8	59
CS-PdPt	4.942	46	40
V-NiFeMo LDH	2.23	80	41
Pt – Co(OH) ₂ /CC	5.7	32	42
YS-Pt-CoP	3.91	48	43
PtCoMo@NC	4.7	26	44
PtCo@NC	2.67	21	60
Pt@mh-3D MXene	2.4	31	61
Pt/HMCS	5.08	46.2	62
Pt SAs/MoO ₂	1.1	14	63
Pt-CoS ₂ /CC	7.3	24	64
Pt-NiFe LDH/CC	1.56	28	65
Pt@DG	1.57	37	66
Pt@NOMC-A	7.2	41	45
Pt@Mn-SAs/N-C	1.98	16	67
Pt ₁ /OLC	0.27	38	68
MoPt ₂ -MoNi ₄ /Mo ₂ C	9.72	53	69
Pt ₃ Fe/BNC	13.2	24	49
Pt ₃ Fe/NMCS-A	10.3	29	50
Pt@CuFe-LDHm	1.1	47	51

References

- [1] J. Fan, X. Ma, J. Xia, L. Zhang, Q. Bi and W. Hao, *J. Colloid Interface Sci.*, 2024, **657**, 393-401.
- [2] Y. Shi, S. Zhou, J. Liu, X. Zhang, J. Yin, T. Zhan, Y. Yang, G. Li, J. Lai and L. Wang, *Appl. Catal. B-Environ. Energy*, 2024, **341**, 123326.
- [3] X. Liu, S. Wei, S. Cao, Y. Zhang, W. Xue, Y. Wang, G. Liu and J. Li, *Adv. Mater.*, 2024, DOI: 10.1002/adma.202405970, e2405970.
- [4] Q. Gao, W. Luo, X. Y. Ma, Z. M. Ma, S. J. Li, F. L. Gou, W. Shen, Y. M. Jiang, R. X. He and M. Li, *Applied Catalysis B-Environment and Energy*, 2022, **310**, 121356.
- [5] C. Lyu, J. R. Cheng, Y. Q. Yang, W. M. Lau, N. Wang, Q. Wu and J. L. Zheng, *J. Colloid Interface Sci.*, 2023, **651**, 93-105.
- [6] Z. Chen, H. Qing, R. Wang and R. Wu, *Energy Environ. Sci.*, 2021, **14**, 3160-3173.
- [7] H. Xu, G. Xu, L. Chen and J. Shi, *Adv Mater*, 2022, **34**, e2200058.
- [8] M. K. Kim, B. Lamichhane, B. Song, S. Kwon, B. Wang, S. Kattel, J. H. Lee and H. M. Jeong, *Applied Catalysis B: Environment and Energy*, 2024, **352**, 124037.
- [9] W. Li, H. Zhang, K. Zhang, W. Hu, Z. Cheng, H. Chen, X. Feng, T. Peng and Z. Kou, *Appl. Catal., B*, 2022, **306**, 121095.
- [10] M. Hu, B. Liu, H. Chen, X. Xu, P. Jing, X. Guo, R. Yang, X. Wang, R. Gao and J. Zhang, *Appl. Catal., B*, 2023, **322**, 122131.
- [11] J. Chen, Y. Ha, R. R. Wang, Y. X. Liu, H. B. Xu, B. Shang, R. B. Wu and H. G. Pan, *Nano Micro Lett.*, 2022, **14**, 186.
- [12] M. Ma, J. Xu, H. Wang, X. Zhang, S. Hu, W. Zhou and H. Liu, *Appl. Catal., B*, 2021, **297**, 120455.
- [13] B. Geng, F. Yan, X. Zhang, Y. He, C. Zhu, S. L. Chou, X. Zhang and Y. Chen, *Adv Mater*,

2021, **33**, e2106781.

- [14] B. Wang, L. Wang, J. H. Lee, T. T. Isimjan, H. M. Jeong and X. Yang, *Carbon Energy*, 2024,
DOI: 10.1002/cey2.526, e526.
- [15] P. Shen, B. Zhou, Z. Chen, W. Xiao, Y. Fu, J. Wan, Z. Wu and L. Wang, *Appl. Catal., B*, 2023,
325, 122305.
- [16] Y. Gao, Z. Chen, Y. Zhao, W. Yu, X. Jiang, M. He, Z. Li, T. Ma, Z. Wu and L. Wang, *Appl.
Catal., B*, 2022, **303**, 120879.
- [17] J. Liu, G. Hodes, J. Yan and S. Liu, *Chin. J. Catal.*, 2021, **42**, 205-216.
- [18] Y. Z. Wu, L. Wang, T. Bo, Z. F. Chai, J. K. Gibson and W. Q. Shi, *Adv. Funct. Mater.*, 2023,
33, 2214375.
- [19] Y. S. Tan, J. R. Feng, L. Q. Kang, L. X. Liu, F. J. Zhao, S. Y. Zhao, D. J. L. Brett, P. R.
Shearing, G. J. He and I. P. Parkin, *Energy Environ. Mater.*, 2023, **6**, e12398.
- [20] P. Chang, S. Zhang, X. Xu, Y. Lin, X. Chen, L. Guan and J. Tao, *Chem. Eng. J.*, 2021, **423**,
130196.
- [21] N. Yao, R. Meng, J. Su, Z. Fan, P. Zhao and W. Luo, *Chem. Eng. J.*, 2021, **421**, 127757.
- [22] Z. Lin, B. Xiao, Z. Wang, W. Tao, S. Shen, L. Huang, J. Zhang, F. Meng, Q. Zhang, L. Gu and
W. Zhong, *Adv. Funct. Mater.*, 2021, **31**, 2102321.
- [23] W. Zhang, Q. Jia, H. Liang, L. Cui, D. Wei and J. Liu, *Chem. Eng. J.*, 2020, **396**, 125315.
- [24] Y. X. Wang, J. Yu, Q. Liu, J. Y. Liu, R. R. Chen, J. H. Zhu, R. M. Li and J. Wang,
ELECTROCHIMICA ACTA, 2023, **438**.
- [25] H. Liu, G. Tan, M. Li, Z. Zhang, M. Getaye Sendeku, Y. Li, Y. Kuang and X. Sun, *Chem. Eng.
J.*, 2023, **458**, 141414.
- [26] J. Xu, X. Wang, X. Mao, K. Feng, J. Xu, J. Zhong, L. Wang, N. Han and Y. Li, *Energy
Environ. Sci.*, 2023, **16**, 6120-6126.

- [27] R. Zhang, H. Liu, C. Wang, L. Wang, Y. Yang and Y. Guo, *ChemCatChem*, 2020, **12**, 3068-3075.
- [28] T. Qiu, J. Cheng, Z. Liang, H. Tabassum, J. Shi, Y. Tang, W. Guo, L. Zheng, S. Gao, S. Xu and R. Zou, *Appl. Catal. B Environ.*, 2022, **316**, 121626.
- [29] D. Chen, Z. Pu, R. Lu, P. Ji, P. Wang, J. Zhu, C. Lin, H. W. Li, X. Zhou, Z. Hu, F. Xia, J. Wu and S. Mu, *Adv. Energy Mater.*, 2020, **10**, 2000814.
- [30] D. Li, X. Chen, Y. Lv, G. Zhang, Y. Huang, W. Liu, Y. Li, R. Chen, C. Nuckolls and H. Ni, *Appl. Catal. B Environ.*, 2020, **269**, 118824.
- [31] J. Zhang, C. Cheng, L. Xiao, C. Han, X. Zhao, P. Yin, C. Dong, H. Liu, X. Du and J. Yang, *Adv. Mater.*, 2024, **36**, 2401880.
- [32] C. Hu, J. Hong, J. Huang, W. Chen, C. U. Segre, K. Suenaga, W. Zhao, F. Huang and J. Wang, *Energy Environ. Sci.*, 2020, **13**, 4249-4257.
- [33] Y. Li, X. Tan, H. Tan, H. Ren, S. Chen, W. Yang, S. C. Smith and C. Zhao, *Energy Environ. Sci.*, 2020, **13**, 1799-1807.
- [34] M. Ning, F. Zhang, L. Wu, X. Xing, D. Wang, S. Song, Q. Zhou, L. Yu, J. Bao, S. Chen and Z. Ren, *Energy Environ. Sci.*, 2022, **15**, 3945-3957.
- [35] L. Deng, S.-F. Hung, S. Zhao, W.-J. Zeng, Z.-Y. Lin, F. Hu, Y. Xie, L. Yin, L. Li and S. Peng, *Energy Environ. Sci.*, 2023, **16**, 5220-5230.
- [36] L. Li, D. Yu, P. Li, H. Huang, D. Xie, C.-C. Lin, F. Hu, H.-Y. Chen and S. Peng, *Energy Environ. Sci.*, 2021, **14**, 6419-6427.
- [37] Y. Dang, T. Wu, H. Tan, J. Wang, C. Cui, P. Kerns, W. Zhao, L. Posada, L. Wen and S. L. Suib, *Energy Environ. Sci.*, 2021, **14**, 5433-5443.
- [38] Q. He, Y. Zhou, H. Shou, X. Wang, P. Zhang, W. Xu, S. Qiao, C. Wu, H. Liu, D. Liu, S. Chen, R. Long, Z. Qi, X. Wu and L. Song, *Adv Mater*, 2022, **34**, e2110604.

- [39] J. Q. Chi, J. Y. Xie, W. W. Zhang, B. Dong, J. F. Qin, X. Y. Zhang, J. H. Lin, Y. M. Chai and C. G. Liu, *ACS Appl Mater Interfaces*, 2019, **11**, 4047-4056.
- [40] B. T. Jebaslinhepzybai, N. Prabu and M. Sasidharan, *Int. J. Hydrogen Energy*, 2020, **45**, 11127-11137.
- [41] J. Li, R. T. Gao, X. Liu, X. Zhang, L. Wu and L. Wang, *ACS Appl Mater Interfaces*, 2023, **15**, 42501-42510.
- [42] Z. Xing, C. Han, D. Wang, Q. Li and X. Yang, *ACS Catal.*, 2017, **7**, 7131-7135.
- [43] Z. Jiang, J. Ren, Y. Li, X. Zhang, P. Zhang, J. Huang, C. Du and J. Chen, *Dalton Trans.*, 2019, **48**, 8920-8930.
- [44] W.-H. Huang, X.-M. Li, D.-Y. Yu, X.-F. Yang, L.-F. Wang, P.-B. Liu and J. Zhang, *Nanoscale*, 2020, **12**, 19804-19813.
- [45] Y. Yin, T. Liu, D. Liu, Z. Wang, Q. Deng, D. Qu, Z. Xie, H. Tang and J. Li, *J. Colloid Interface Sci.*, 2018, **530**, 595-602.
- [46] K. M. Naik, E. Higuchi and H. Inoue, *Nanoscale*, 2020, **12**, 11055-11062.
- [47] Y. Qiu, Z. Wen, C. Jiang, X. Wu, R. Si, J. Bao, Q. Zhang, L. Gu, J. Tang and X. Guo, *Small*, 2019, **15**, e1900014.
- [48] C. Zhang, P. Wang, W. Li, Z. Zhang, J. Zhu, Z. Pu, Y. Zhao and S. Mu, *J. Mater. Chem. A*, 2020, **8**, 19348-19356.
- [49] Y. Qiao, J. Cui, F. Qian, X. Xue, X. Zhang, H. Zhang, W. Liu, X. Li and Q. Chen, *ACS Appl. Nano Mater.*, 2021, **5**, 318-325.
- [50] P. Kuang, Z. Ni, B. Zhu, Y. Lin and J. Yu, *Adv. Mater.*, 2023, **35**, 2303030.
- [51] J. Song, J.-L. Chen, Z. Xu and R. Y.-Y. Lin, *Chem. Commun.*, 2022, **58**, 10655-10658.
- [52] K. Jiang, B. Liu, M. Luo, S. Ning, M. Peng, Y. Zhao, Y.-R. Lu, T.-S. Chan, F. M. F. de Groot and Y. Tan, *Nat. Commun.*, 2019, **10**, 1743.

- [53] M. Yi, S. Hu, B. Lu, N. Li, Z. Zhu, X. Huang, M. Wang and J. Zhang, *J. Alloys Compd.*, 2021, **884**, 161042.
- [54] Z. Pu, R. Cheng, J. Zhao, Z. Hu, C. Li, W. Li, P. Wang, I. S. Amiinu, Z. Wang, W. Min, D. Chen and S. Mu, *iScience*, 2020, **23**, 101793.
- [55] N. Wang, X. Bo and M. Zhou, *ACS Appl Mater Interfaces*, 2022, DOI: 10.1021/acsami.2c00747.
- [56] M. Li, Y. Zhu, N. Song, C. Wang and X. Lu, *J. Colloid Interface Sci.*, 2018, **514**, 199-207.
- [57] J. Xu, M. Zhong, N. Song, C. Wang and X. Lu, *Chin. Chem. Lett.*, 2023, **34**, 107359.
- [58] M. Liu, G. Lv, H. Liu, T. Liu, L. Kong and L. Liao, *Chin. Chem. Lett.*, 2024, **35**, 108459.
- [59] C. Zhang, X. Liang, R. N. A. Xu, C. N. Dai, B. Wu, G. Q. Yu, B. H. Chen, X. L. Wang and N. Liu, *Adv. Funct. Mater.*, 2021, **31**, 2008298.
- [60] M. Zhang, T. Zhou, D. Bukhvalov, F. Han, C. Wang and X. Yang, *Appl. Catal., B*, 2023, **337**, 122976.
- [61] L. Xiu, W. Pei, S. Zhou, Z. Wang, P. Yang, J. Zhao and J. Qiu, *Adv. Funct. Mater.*, 2020, **30**, 1910028.
- [62] X. K. Wan, H. B. Wu, B. Y. Guan, D. Luan and X. W. D. Lou, *Adv Mater*, 2020, **32**, e1901349.
- [63] Y. Qiu, S. Liu, C. Wei, J. Fan, H. Yao, L. Dai, G. Wang, H. Li, B. Su and X. Guo, *Chem. Eng. J.*, 2022, **427**, 131309.
- [64] X. Han, X. Wu, Y. Deng, J. Liu, J. Lu, C. Zhong and W. Hu, *Adv. Energy Mater.*, 2018, **8**, 1800935.
- [65] Q. Yan, P. Yan, T. Wei, G. Wang, K. Cheng, K. Ye, K. Zhu, J. Yan, D. Cao and Y. Li, *J. Mater. Chem. A*, 2019, **7**, 2831-2837.
- [66] Q. Yang, H. Liu, P. Yuan, Y. Jia, L. Zhuang, H. Zhang, X. Yan, G. Liu, Y. Zhao, J. Liu, S. Wei, L. Song, Q. Wu, B. Ge, L. Zhang, K. Wang, X. Wang, C. R. Chang and X. Yao, *J Am*

Chem Soc, 2022, **144**, 2171-2178.

- [67] L. Gong, J. Zhu, F. Xia, Y. Zhang, W. Shi, L. Chen, J. Yu, J. Wu and S. Mu, *ACS Catal.*, 2023, **13**, 4012-4020.
- [68] D. Liu, X. Li, S. Chen, H. Yan, C. Wang, C. Wu, Y. A. Haleem, S. Duan, J. Lu, B. Ge, P. M. Ajayan, Y. Luo, J. Jiang and L. Song, *Nat. Energy*, 2019, **4**, 512-518.
- [69] H. Zhang, P. Song, P. Yao, D. Zhang, J. Cao, X. Gong, C. Han and W. Xu, *Chem. Eng. J.*, 2023, **470**, 144375.